DOI: 10.13009/EUCASS2025-662
11TH EUROPEAN CONFERENCE FOR AERONAUTICS AND SPACE SCIENCES (EUCASS)

Similitude Relationships and Scaling in Aircraft Icing

Mehmet Harun Özkanaktı[⋆] *and Serkan Özgen*[⋆†]
[⋆]*Middle East Technical University, Department of Aerospace Engineering*
Dumlupınar Bul. 1, 06800, Çankaya, Ankara, Türkiye
hozkanakti@gmail.com · serkan.ozgen@ae.metu.edu.tr
[†]Corresponding author

Abstract

Aircraft icing has become increasingly important due to its critical impact on flight safety. Experimental investigation of icing phenomena requires reduced-scale models tested in icing wind tunnels, as real-size testing is mostly impractical and not feasible. Achieving accurate similitude between model and full-scale conditions requires replicating key parameters such as flow field, droplet trajectories, impingement pattern, water catch and thermodynamics of ice accretion. Several scaling methods have been proposed, among which the Modified Ruff Method provides a framework for icing physics by matching six dimensionless parameters.
This paper aims to investigate the phenomena related to similitude and scaling in aircraft icing using an in-house computational tool that predicts ice accretion based on the Extended Messinger Model. Validation results presented cover a wide range of icing conditions, namely rime, glaze, and beak ice extending into the compressible-flow regime.

1 Introduction

The risk of icing corresponds to degraded aerodynamic and overall performance of the aircraft, reduction in stability, and eventually compromised flight safety. Moreover, and most importantly, icing can lead to the malfunction of critical equipment, instruments, and engine failure. The phenomenon of icing in aviation is becoming increasingly important as the number of accidents or incidents in this field increases over time. In order to understand icing conditions and mitigate their adverse effects, it is necessary to study and test the conditions that cause icing. The icing wind tunnel, one of the most crucial test environments, is required to conduct studies in this field. In order to utilise the icing tunnel, it is essential to dimension the model to be placed in the tunnel and to create the equivalent icing conditions as in natural icing conditions by varying the size of the model and icing parameters. However, it is not feasible to place a full-size model in an icing wind tunnel because there are few wind tunnels of this size, and even if a wind tunnel of this size is available, the operating costs are high. For these reasons, the model should be reduced to smaller than the actual dimensions and rendered suitable for the wind tunnel test chamber. This requires varying flight and icing conditions so that an equivalent icing environment is created.

In order to serve this purpose, this study aims to develop a methodology for scaling a reference icing case and comparing this with a scaled case with outcomes of an in-house ice accreation computational tool. Understanding the physical phenomena of icing physics makes it possible to implement this process in an appropriate manner. The method involves maintaining the similitude of a number of dimensionless parameters governed by icing physics between reference and scaled conditions.

The primary factors influencing atmospheric icing are the ambient temperature (T_∞), size distribution of droplets in clouds often represented by the cloud median volume diameter (MVD), free-stream velocity (V_∞) and liquid-water content (LWC). The size distribution of droplets is responsible for the trajectories and impingement patterns of the droplets contacting the object. Therefore, it is crucial to study ice accumulation and the effects of the droplet size and their trajectories on ice growth physics.

In previous studies, various methods have been used to gather scaled ice shape formations corresponding to reference ice shape formations. The similarities to be established in the scaling analysis are geometric similarity, flow-field similarity, droplet trajectory similarity, water catch similarity, energy balance similarity, and surface water dynamics similarity. To this end, different scaling parameters for icing have been proposed depending on the similitude requirements to be met. It is important to note that all of these scaling approaches are based on various combinations of the modified inertia parameter, K_0; accumulation parameter, A_c; freezing fraction, n_0; Weber number, We; drop energy

DOI: 10.13009/EUCASS2025-662

parameter, ϕ; and air energy transfer parameter, θ, to achieve similitude. These parameters will be discussed in greater detail below. Notable icing scaling methods have been proposed, which are combinations of similitudes of droplet trajectory, water catch, and energy balance. Different combinations of energy balance parameters provide the similarity of the energy balance. Various suggested scaling methods involve different numbers of similarity parameters such as K_0 and A_c constant; K_0, A_c, and n_0 constant; K_0, A_c, n_0, b constant; and K_0, A_c, n_0, ϕ and θ constant.

Sibley and Smith proposed a new scaling method, which comprises a set of parameters to be matched in terms of similitudes of droplet trajectory, water catch, and energy balance. These parameters can also be expressed in terms of icing physics notation as K_0, A_c, n_0, b [1].

Numerous empirical studies conducted in the NASA Glenn Icing Research Tunnel have demonstrated compelling outcomes. The similitude was provided by the similarity of geometry, energy balance, droplet trajectory, flow field, water catch, and surface water dynamics [2]. These similitude parameters are used for scaling test conditions in this intensive work, and the effects of the scaling parameters on the final geometry of the ice shape and the physical phenomena containing the icing parameters were deduced.

A novel scaling method was proposed by Ruff [3] where scaled and full-scale versions of cylinder and airfoil sections were studied. As a result of this work, ice accumulation on the specimen was compared to real-case conditions to prove the accuracy of the scaling method. The Modified Ruff Method was proposed with a constant Weber number approach to compute velocity and obtain reference ice shape with a scaled size model. This method requires tuning of energy balance, water catch, surface water dynamics, the droplet trajectory, as well as scaling of the geometry and angle of attack [3]. This method is also employed in the current study.

A study reported by Anderson [4] suggests that the conclusive method is the most precise to obtain the proper outer geometry of scaled ice shapes. The limitation of the scaling method is the airflow velocity since the velocities leading to a Reynolds number of less than 2×10^5 and beyond the critical Mach number have unique characteristics that only allow scaling with further work. A scaling method is developed by identifying the scaling parameters, analysing icing and similitude physics in the airflow and gathering the knowledge from previous studies on icing scaling methods.

In the present study, the primary intention is to include the effect of surface water dynamics, which is contained in the scaling method by matching the Weber number We through implementation of *Modified Ruff Method*. The scaling parameters to be matched are determined as K_0, A_c, n_0, ϕ, θ and We_L for tunnels with altitude adjustment capability.

Icing effects must be assessed early in design and verified for certification. Both FAA and EASA define icing envelopes in 14 CFR Part 25 and CS-25 Appendices C, O and P [5–7]. Computational analyses guide preliminary design, but final approval requires tunnel or flight tests that reproduce real icing conditions. This study applies scaling methods to a reference icing scenario, evaluates the fidelity of model-scale predictions against full-scale data, and identifies the limitations inherent in current similitude practices.

In the first part of the study, the modelling and scaling approach is summarised. Under the same title, the formulation and definitions of the similitude approach are given. Then, in the Methodology section, the details of the scaling method and the implementaion of the Modified Ruff Method are explained. In the Results and Discussion section, the results of the simulation analysis for the reference and scaled cases are presented and obtained data are compared. In these cases, the effects of the parameters determining the similitude on the results are discussed. At the end of the study, the limitations and capabilities of the study are summarized.

2 Modelling & Scaling Approach

The prediction of atmospheric ice formation, which is one of the critical issues in the field of aviation and has a significant role in many accidents and incidents, can be predicted by numerical methods. Although numerical methods give valuable information about this issue, the accuracy of these methods should be validated by experimental methods. Icing experiments can be done using one of two methods: flight test and the wind tunnel test. The most accurate and reliable testing is the flight test. However, this testing method is too expensive and risky to run, and besides, it is hard to encounter natural icing conditions with the desired severity. The second alternative is testing in icing wind tunnels, which have inherent limitations related to model size, air speed and icing conditions. When a full-scale model is too large for an existing wind tunnel facility or required test conditions exceed the operational limitations of the facility, a scaling method is required to provide scaled ice accretions for the desired test conditions. To ensure test reliability, the scaling method must be utilized for icing conditions prior to wind tunnel testing, respecting similitude principles.

DOI: 10.13009/EUCASS2025-662

2.1 Similitude and Scaling Analysis, Modified Ruff Method

The scaling models include size scaling and scaling of icing conditions. Icing conditions similitude is established by providing similitude of flow field, droplet trajectories, impingement pattern, water catch and thermodynamics of ice accretion process. Several scaling methods have been proposed, which are combinations of similitudes of droplet trajectory, water catch and energy balance. One such method is the Modified Ruff Method, which requires adjustment of energy balance, water catch, surface water dynamics, droplet trajectory, as well as modelling of the non-dimensional geometry and angle of attack [4]. The method involves matching six dimensionless parameters in the reference and scaled conditions as summarized in Figure 1. This method is outlined in the following sections.

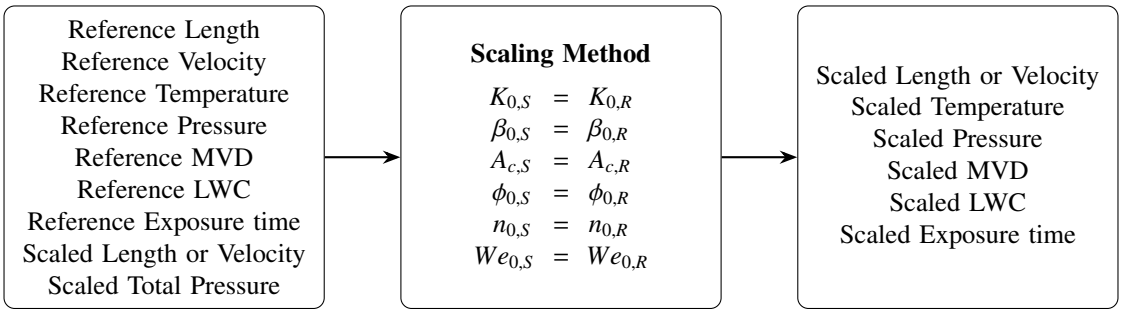

Figure 1: Summary of Modified Ruff Method

2.1.1 Geometric Similarity

The geometries in the reference and scaled models must be geometrically similar over the entire model. If the reference geometry is an airfoil, the scaled geometry must be the same airfoil, scaled down by an appropriate amount. As ice grows on the model, the shape must continue to be similar for flowfield similarity to be maintained.

2.1.2 Flowfield Similarity

Flowfield similarity requires that the Reynolds and Mach numbers for the scaled test need to be matched to their respective full-size, or reference, values. The definitions for these parameters are [4]:

$$Re_a = \frac{\rho V_\infty d}{\mu} \tag{1}$$

$$M = \frac{V_\infty}{\sqrt{\gamma R T_\infty}} \tag{2}$$

In eq. (1), the length scale d represents either the diameter if the model is a cylinder or twice the leading edge radius if the model is an airfoil. For many analyses, the chord of the airfoil has been chosen as the characteristic length; however, ice accretion occurs mainly near the leading edge region. Therefore, in studying scaling similarity it seems reasonable to define similarity parameters in terms of a length scale representative of the leading-edge region [4].

Icing occurs in the atmosphere only within a limited range of temperatures (−40° - 0°C). Thus, because γ and R are constant properties of air, equating the Mach number for the scaled and reference cases requires that the velocities for the two cases be very nearly the same. However, to match the Reynolds numbers when the scale model is, for example, half the reference size, it is necessary for the scaled velocity to be approximately double the reference velocity. Clearly, then, Mach and Reynolds numbers cannot be simultaneously matched when the scale model is other than full size [4]. Thus, for most scaling analyses matching the Mach Number and Reynolds Number is not aimed. This might be justified considering the fact that in majority of the icing conditions, the Mach number is relatively low, hence compressibility effects are negligible and ice accretion occurs near the stagnation regions where the boundary layer is thin and viscous effects are small. Therefore, the similarity of flow field is considered to be achieved when the Mach number and Reynolds number is in the interval $M@Re = 2 * 10^5 < M < M_{critical}$ near the stagnation region. Lower limit corresponds to a Reynolds number that the velocity distribution is preserved up to stall and upper limit corresponds to the critical Mach number [3].

DOI: 10.13009/EUCASS2025-662

2.1.3 Droplet Trajectory Similarity

For droplet trajectory similitude, droplet trajectories and the impingement zones should be matched between the reference and scaled conditions. This requires K_o and β_o to be matched between the two conditions [4]:

$$K_{0,reference} = K_{0,scaled} \tag{3}$$

For the modified inertia parameter, Langmuir and Blodgett's expression is used [8]:

$$K_0 = \frac{1}{8} + \frac{\lambda}{\lambda_{Stokes}}\left(K - \frac{1}{8}\right) \quad \text{for } K > \frac{1}{8} \tag{4}$$

where, K is the non-dimensional inertia parameter [8]:

$$K = \frac{\rho_w V_\infty (\text{MVD})^2}{18 d \mu} \tag{5}$$

where d is the airfoil leading edge diameter and ρ_w denotes density of water. The drop-range factor is [4]:

$$\frac{\lambda}{\lambda_{Stokes}} = \frac{1}{0.8388 + 0.001483 Re_d + 0.1847\sqrt{Re_d}} \tag{6}$$

where Re_d is the Reynolds number based on median droplet volumetric diameter:

$$Re_d = \frac{\rho V_\infty \,\text{MVD}}{\mu} \tag{7}$$

Finally, stagnation-line collection efficiency is given by:

$$\beta_0 = \frac{1.40\left(K_0 - \frac{1}{8}\right)^{0.84}}{1 + 1.40\left(K_0 - \frac{1}{8}\right)^{0.84}} \tag{8}$$

2.1.4 Water Catch Similarity

The amount of ice accreted relies on the amount of water striking the surface. Water catch parameters should be matched in order to ensure ice accretion similitude. The freezing fraction concept, n, is introduced by Messinger [9]. For particular conditions, there is no local freezing of water; in that case, the n parameter is equal to zero. Otherwise, if all water droplets freeze on impact, the n parameter should be equal to 1. In intermediate cases where freezing occurs partially upon impact, $0 < n < 1$.

In the following equation, n is taken as one:[4]

$$\frac{d\Delta}{dt} = \frac{\dot{m}}{\rho_i} \tag{9}$$

The total mass of water impinging in a unit area per unit time is given as in eq. (10),

$$\dot{m} = \beta V_\infty \text{LWC} \tag{10}$$

Integrating over exposure time t_{exp},

$$\Delta = \frac{\beta V_\infty \text{LWC} t_{exp}}{\rho_i} \tag{11}$$

and enforcing similarity,

$$\left(\frac{\Delta}{d}\right)_{reference} = \left(\frac{\Delta}{d}\right)_{scaled} \quad \Longrightarrow \quad \left(\frac{\beta V_\infty \text{LWC} t_{exp}}{\rho_i d}\right)_{reference} = \left(\frac{\beta V_\infty \text{LWC} t_{exp}}{\rho_i d}\right)_{scaled} \tag{12}$$

The accumulation parameter, A_c needs to be matched between reference and scaled conditions [4]:

$$A_{c,reference} = A_{c,scaled} \tag{13}$$

where,

$$A_c = \frac{\text{LWC}\, V_\infty\, t_{exp}}{\rho_i d} \tag{14}$$

DOI: 10.13009/EUCASS2025-662

2.1.5 Energy Balance Similarity

Ice accretion occurs when the supercooled droplets impinge on the surface and either freeze entirely (rime ice) or partially (glaze ice). Ice accretes near the stagnation point so the energy balance is established at this location. Although the energy balance similitude is not required for rime ice, it is required in glaze ice in order to calculate the freezing fraction parameter n_o. When the freezing fraction at the stagnation point is less than 0, it means that ice accretion does not occur at the stagnation point but occurs elsewhere. For similitude, freezing fraction parameter n_o is to be matched between reference and scaled conditions [4]:

$$n_{o,reference} = n_{o,scaled} \tag{15}$$

where

$$n_o = \left(\frac{C_{pw}}{L_F}\right)\left(\phi + \frac{\theta}{b}\right) \tag{16}$$

In the above equation, b is known as the relative heat factor introduced by Tribus et al [10]:

$$b = \frac{V_\infty \beta_o C_{pw} \mathrm{LWC}}{h_{co}} \tag{17}$$

where h_{co} is the convective heat transfer coefficient at the stagnation point calculated from:

$$Nu = \frac{h_{co} d}{k} \tag{18}$$

where k is the thermal conductivity. Nusselt number, Nu can be calculated from:

$$Nu = 1.14 Pr^{0.4} Re^{0.5} \tag{19}$$

where Pr is the Prandtl number. Parameters ϕ and θ are known as the drop energy transfer and air energy transfer parameters, respectively [10]:

$$\phi = T_f - T_\infty - \frac{V_\infty^2}{2C_{pw}} \tag{20}$$

$$\theta = \left(T_f - T_\infty - \frac{V_\infty^2}{2C_p}\right) + \frac{h_g}{h_{co}}\left(\frac{\frac{p_{ww}}{T_\infty} - \frac{P_{t\infty}}{T_{t\infty}}\frac{p_w}{p_\infty}}{\frac{1}{0.622}\frac{P_{t\infty}}{T_{t\infty}} - \frac{p_{ww}}{T_\infty}}\right) L_E \tag{21}$$

In the above equation, h_g is the gas phase mass transfer coefficient calculated from:

$$h_g = \frac{h_{co}}{C_p}\left(\frac{Pr}{Sc}\right)^{0.67} \tag{22}$$

where Sc is the Schmidt number. Also, the parameters p_w and p_{ww} are the vapor pressure of water in the atmosphere and vapor pressure of water over water, respectively, which can be calculated using:

$$p_w = a_o + \Delta T(a_1 + \Delta T(a_2 + \Delta T(a_3 + \Delta T(a_4 + \Delta T(a_5 + \Delta T a_6))))) \tag{23}$$

with

$$\begin{aligned} \Delta T &= T - 273.15 \\ a_0 &= 610.78 Pa \\ a_1 &= 44.365 Pa/K \\ a_2 &= 1.4289 Pa/K^2 \\ a_3 &= 2.6506 * 10^{-2} Pa/K^3 \\ a_4 &= 3.0312 * 10^{-4} Pa/K^4 \\ a_5 &= 3.0341 * 10^{-6} Pa/K^5 \\ a_6 &= 6.1369 * 10^{-9} Pa/K^6 \end{aligned} \tag{24}$$

Equation (23) can be used to compute both the vapor pressure of water over water (p_{ww}) and that in the atmosphere (p_w), by substituting the appropriate temperature ΔT. Finally, $P_{t\infty}$ and $T_{t\infty}$ are the total pressure and total temperature of the flow, respectively.

DOI: 10.13009/EUCASS2025-662

2.1.6 Surface Water Dynamics

In glaze ice conditions, a water film is present over an ice layer. The flow of this water film as runback water has an effect on the accreted ice (runback ice). The similitude of the behaviour of this water film requires Weber number We, to be matched between the reference and scaled models [4]:

$$We_{reference} = We_{scaled} \tag{25}$$

where the Weber number is defined as:

$$We = \frac{V_\infty^2 d\rho}{\sigma_{wa}} \tag{26}$$

where, σ_{wa} is the surface tension between water and air. The freestream velocity similitude between scaled and reference cases is established by the below equality:

$$V_{\infty,scaled} = V_{\infty,reference}\left(\frac{d_{reference}}{d_{scaled}}\right)^{\frac{1}{2}} \tag{27}$$

3 Methodology

A set of icing cases with published experimental data were selected to encompass rime, glaze and beak ice conditions. This selection targeted to evaluate both the numerical limitations and physical constraints of the simulation framework. Each reference case is initially computed at full scale in order to obtain the reference ice shape and collection efficiency distribution. Subsequently, similitude analysis was performed to determine the scaled conditions for a 50% scaled model. Finally, ice shape and collection efficiency distribution are computed for the scaled condition. Ice shapes and droplet collection efficiencies are computed using an in-house computational tool that predicts ice accretion based on the Extended Messinger Model [11].

Data from three DRA/NASA/ONERA cases (27, 30, 39) represent rime, glaze and beak ice conditions, respectively [12]. Physical conditions and similitude parameters appear in Table 1 while computed collection-efficiency distributions and final ice shapes are shown in Results & Discussion section.

3.1 Implementation of the Modified Ruff Method

In the current study, the Modified Ruff Method is implemented with the following steps:

1. **Calculation of Reference Dimensionless Parameters:**
   Initially, the six dimensionless parameters K_0, β_0, A_c, n_0, ϕ, and We, are computed for the full-scale reference case based on known flight conditions and geometry.
2. **Scaling of Freestream Velocity V_∞:**
   Using the selected chord length scale, the scaled freestream velocity V_∞ is calculated by matching the Weber number with the chosen scale ratio $d_{scaled}/d_{reference}$. Equation (27) is solved for $V_{\infty,scaled}$.
3. **Scaling of Static Temperature T_∞:**
   The scaled freestream static temperature is then computed to match the energy balance similarity parameter ϕ. This step guarantees that the thermal characteristics governing heat transfer and phase change are preserved in the scaled model. Matching energy balance similarity parameter ϕ, $T_{\infty,scaled}$ is computed from eq. (20).
4. **Scaling of Median Volume Diameter (MVD):**
   The scaled MVD is calculated iteratively to satisfy the equality of K_0 from eq. (3), which also ensures matching β_0 in eq. (8). This step is essential for accurately replicating droplet trajectory, impingement pattern and collection efficiency behavior on the model surface.
5. **Scaling of Static Pressure p_∞:**
   Taking the total pressures $P_{t\infty}$ equal in the reference and scaled conditions, scaled static pressure $p_{\infty,scaled}$ is obtained.
6. **Scaling of Liquid Water Content (LWC):**
   Establishing the freezing fraction parameter n_o equality in eq. (16), allows scaled LWC to be computed. This step also requires utilization of relative heat factor b and air energy transfer parameter θ in eq. (17) and eq. (21).

DOI: 10.13009/EUCASS2025-662

7. **Scaling of Exposure Time t_{exp}:**
   Finally, the scaled exposure time is computed using the accumulation parameter A_c. This ensures that the total mass of accreted ice on the scaled model corresponds to that of the reference case over equivalent flow-exposure conditions. Matching the accumulation parameter A_c by utilizing eq. (13), yields the icing duration $t_{exp,scaled}$ in scaled conditions.

By rigorously following this sequence, the Modified Ruff Method provides a validated and robust framework for scaling aircraft icing conditions to wind tunnel test environments. The method enables the study of complex icing phenomena at reduced cost and within the practical constraints of available test facilities, while maintaining fidelity to the underlying physical processes.

4 Results & Discussion

In order to demonstrate the validity of the method, a group of test cases that can show the variation of multiple parameters and have experimental literature data were identified. Three DRA/NASA/ONERA icing cases were selected as shown in Table 1 [12]. They represent rime, glaze and beak ice, with widely varying temperature, speed, LWC and exposure times. Each reference case is first computed at full scale for corresponding ice shapes and droplet collection efficiencies. Then, the Modified Ruff algorithm is utilized in order to compute the scaled conditions for a 50% scaled model. Finally, the ice shapes and collection efficiencies are calculated for the scaled problem.

Table 1: Test cases studied for model validation[12]

Case no.	**airfoil**	**chord** $c(m)$	**aoa** $\alpha(^\circ)$	**airspeed** $V_\infty(m/s)$	**temp.** $T_\infty(^\circ\text{C})$	**pressure** p_{st} (kPa)	**LWC** $\rho_a(g/m^3)$	**drop diam.** $d_p(\mu\text{m})$	**exposure** $t_{exp}(s)$
27	NACA 0012	0.530	4.0	58.1	−27.8	95.61	1.30	20	480
30	NACA 0012	0.530	4.0	58.1	−6.7	95.61	1.30	20	480
39	NACA 0012	0.465	8.0	131.5	−3.9	85.00	0.60	20	180

4.1 Case 27 – Rime Ice

When the method outlined above is applied to Case 27 (rime ice) conditions for a 50% scaled down airfoil, the scaled conditions are obtained as summarized in Table 2[13]. Similitude parameters for Case 27 are given in Table 3. In this case, temperature and velocity are low, typical of rime ice conditions. Also, the flow can be regarded as incompressible. The extent at which the six dimensionless parameters is matched can be seen in Table 3. It can be seen that all six parameters are perfectly matched, therefore one may expect good agreement between reference and scaled results.

Table 2: Case 27 (rime ice) reference and scaled conditions, NACA 0012 airfoil

Type	**chord** $c(m)$	**aoa** $\alpha(^\circ)$	**temperature** $T_\infty(^\circ\text{C})$	**velocity** $V_\infty(m/s)$	**drop. diam.** $d_p(\mu\text{m})$	**LWC** $\rho_a(g/m^3)$	**exp. time** $t_{exp}(s)$	**pressure** p_{st} (kPa)
Reference	0.530	4°	−27.8	58.10	20.0	1.30	480.0	95.61
Scaled	0.265	4°	−28.2	82.17	11.4	1.47	149.8	93.34

Table 3: Case 27 (rime ice) similitude parameters

Type	$\mathbf{K_0}$	β_0	$\mathbf{A_c}$	$\mathbf{n_0}$	**b**	ϕ	θ	**Re**	We	**M**
Reference	1.803	0.684	2.449	1.141	0.576	27.4	36.3	84 492	780 959	0.185
Scaled	1.803	0.684	2.449	1.141	0.555	27.4	35.0	58 501	780 959	0.262

The computations are repeated for the reference and the scaled cases, and the results are summarized in Figure 2 for ice shapes and Figure 3 for collection efficiencies. As can be seen, an almost perfect agreement is observed both for the collection efficiency distributions and the ice shapes. This is an expected outcome because in rime ice formation, only droplet trajectory similarity and water catch similarity play a role, while energy balance similarity and surface water dynamics similarity have negligible, if any, contribution.

DOI: 10.13009/EUCASS2025-662

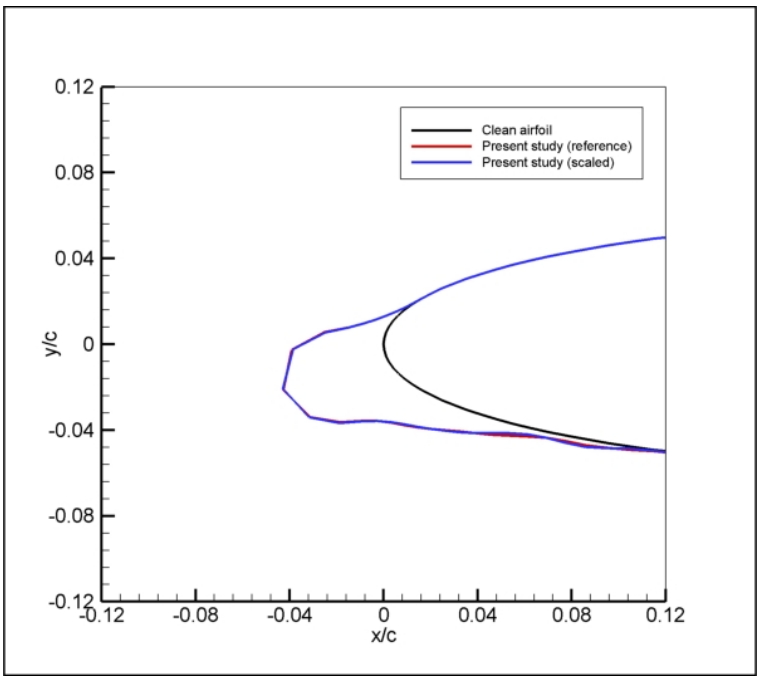

Figure 2: Ice shapes for reference and scaled rime ice conditions, Case 27

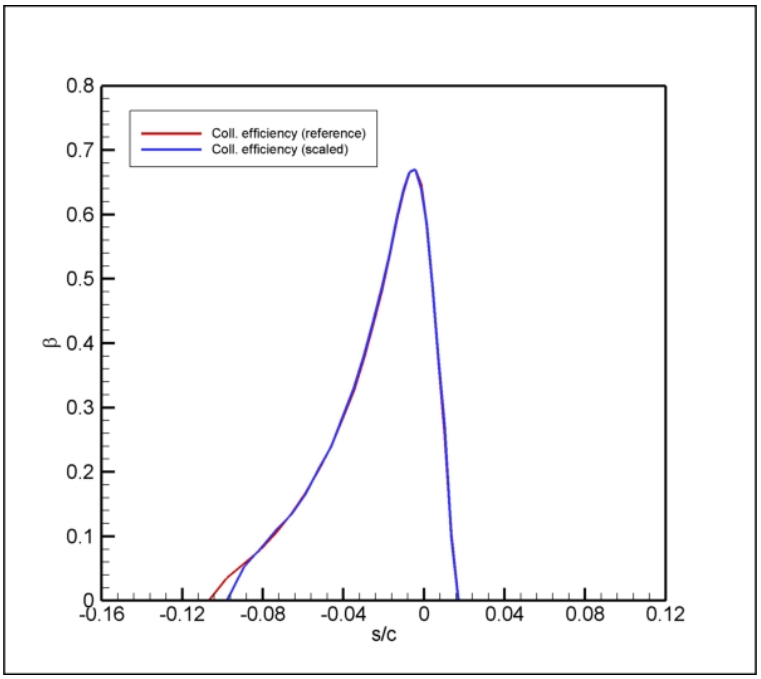

Figure 3: Collection efficiencies for reference and scaled rime ice conditions, Case 27

4.2 Case 30 - Glaze Ice

When the method outlined above is applied this time to Case 30 (glaze ice) conditions again for 50% scaled down airfoil, the scaled condition is obtained as summarized in Table 4 [13]. In this case, the temperature is higher, therefore glaze ice formation is expected. The extent at which the six dimensionless parameters is matched can be seen in Table 5. From the table, it can be seen that all six parameters are perfectly matched, therefore one may expect good agreement between reference and scaled results.

DOI: 10.13009/EUCASS2025-662

Table 4: Case 30 (glaze ice) reference and scaled conditions, NACA 0012 airfoil

Type	**chord** $c(m)$	**aoa** $\alpha(°)$	**temperature** $T_\infty(°C)$	**velocity** $V_\infty(m/s)$	**drop. diam.** $d_p(\mu m)$	**LWC** $\rho_a(g/m^3)$	**exp. time** $t_{exp}(s)$	**pressure** p_{st} (kPa)
Reference	0.530	4°	−6.7	58.10	20.0	1.30	480.0	95.61
Scaled	0.265	4°	−7.1	82.17	11.4	1.32	167.3	93.52

Table 5: Case 30 (glaze ice) similitude parameters

Type	$\mathbf{K_0}$	β_0	$\mathbf{A_c}$	$\mathbf{n_0}$	**b**	ϕ	θ	**Re**	We	**M**
Reference	1.782	0.682	2.450	0.284	0.573	6.30	9.27	72 823	780 959	0.178
Scaled	1.782	0.682	2.450	0.284	0.494	6.30	8.00	50 504	780 959	0.251

The results of the computations for collection efficiency distribution and final ice shapes are presented in Figure 4 and Figure 5 for this case. An almost perfect agreement of the collection efficiency distributions is obtained, while the agreement of the ice shapes is also very good. The prominent horn on the upper surface is captured both in reference and scaled conditions. Although the size of the horn is similar in both computations, its angle is predicted slightly differently in the two computations. Considering that this is a glaze ice case, it can be concluded that Modified Ruff Method scales different icing conditions rather faithfully. In addition to trajectory similarity and water catch similarity, apparently energy balance similarity and surface water dynamics similarity are also well-represented. The two latter effects do play a significant role in this case, since water partially freezes and runs back, which are important phenomena in glaze ice conditions.

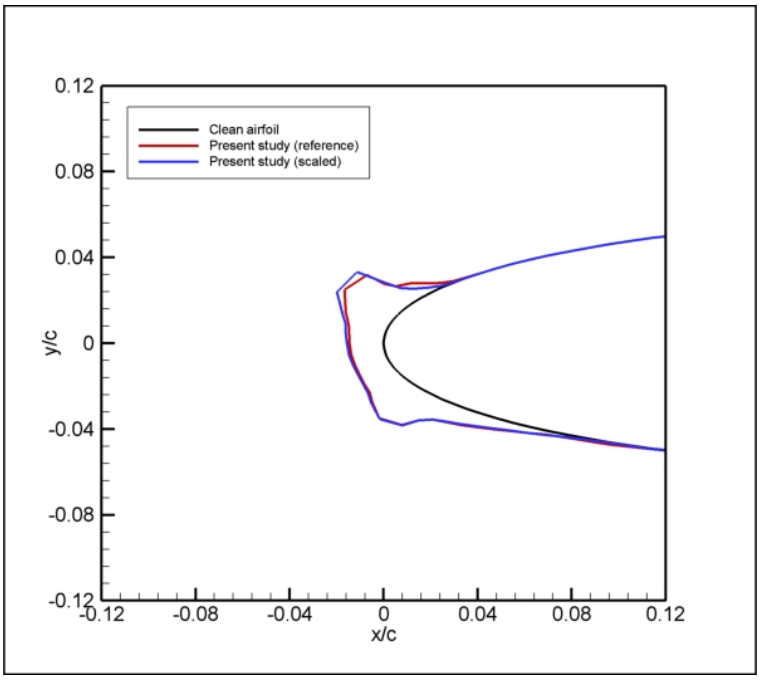

Figure 4: Ice shapes for reference and scaled glaze ice conditions, Case 30

DOI: 10.13009/EUCASS2025-662

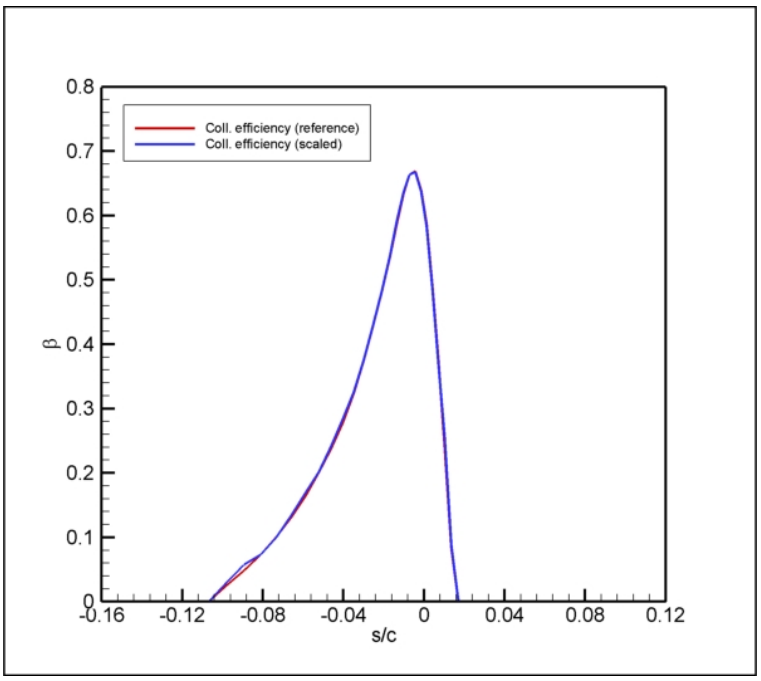

Figure 5: Collection efficiencies for reference and scaled glaze ice conditions, Case 30

4.3 Case 39 - Beak Ice

Finally, the method is applied to beak ice conditions, namely Case 39. In this case, the airfoil is scaled down again by 50%. The reference and scaled conditions are summarized in Table 6. The extent at which the six dimensionless parameters is matched can be seen in Table 7. From the table, it can be seen that all six parameters are perfectly matched, therefore one may expect good agreement between reference and scaled results.

This is a more challenging test case compared to the previous ones because, the angle of attack is rather high, $\alpha = 8°$ and more importantly the freestream velocity value of $V_\infty = 131.5\ m/s$ corresponds to a freestream Mach number of $M = 0.4$, which is above the generally accepted upper limit of $M = 0.3$ for incompressible flow. Moreover, in the scaled conditions, the freestream velcoity value becomes $V_\infty = 186\ m/s$ corresponding to $M = 0.568$, placing it well within compressible flow range. High-speed flow effects are partially accounted for through Prandtl-Glauert compressibility correction in the Panel Method solutions, in the current solution methodology [14].

Table 6: Case 39 (beak ice) reference and scaled conditions, NACA 0012 airfoil

Type	**Chord,** $c(m)$	**aoa,** $\alpha(°)$	**Temperature,** $T_\infty(°\text{C})$	**Velocity,** $V_\infty(m/s)$	**Drop. Diam.,** $d_p(\mu\text{m})$	**LWC,** $\rho_a(g/m^3)$	**Exp. time,** $t_{exp}(s)$	**Pressure,** p_{st} (kPa)
Reference	0.465	8°	−3.9	131.5	20.0	0.60	180.0	85.00
Scaled	0.2325	8°	−5.9	186.0	11.1	2.50	15.3	75.96

Table 7: Case 39 (beak ice) similitude parameters

Type	$\mathbf{K_0}$	β_0	$\mathbf{A_c}$	$\mathbf{n_0}$	**b**	ϕ	θ	**Re**	We	**M**
Reference	3.426	0.791	1.094	−0.042	0.460	1.85	−2.38	126 175	3 509 981	0.400
Scaled	3.426	0.791	1.094	−0.042	1.702	1.85	−8.82	80 828	3 509 981	0.568

Despite this concern, the results presented in Figure 6 and Figure 7 are encouraging. Both the collection efficiency and the ice shape results are in very good agreement between reference and scaled cases. The freestream Mach number of $M = 0.568$ is below the critical Mach number, $M_{critical}$ and the flowfield similarity is established in the computations in addition to trajectory similarity, water catch similarity, energy balance similarity and surface water dynamics similarity.

DOI: 10.13009/EUCASS2025-662

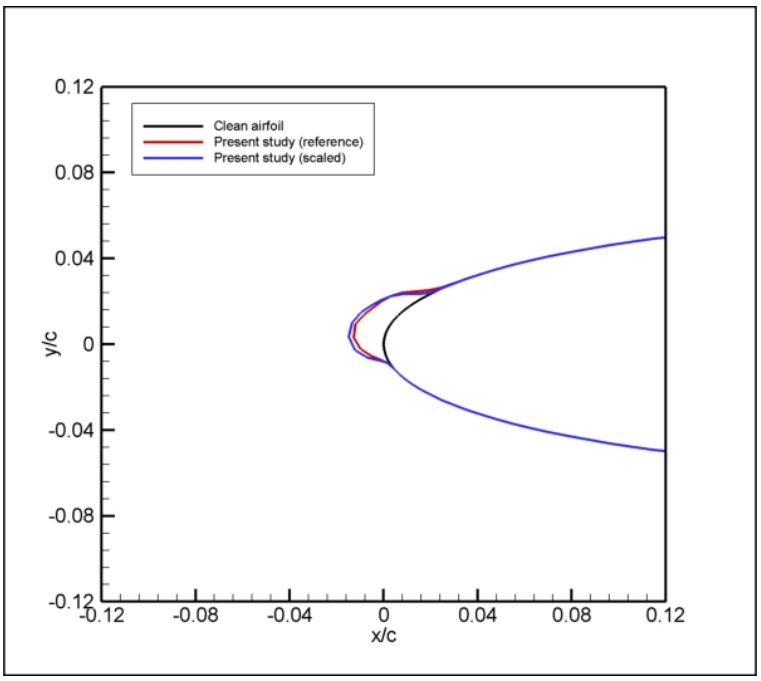

Figure 6: Ice shapes for reference and scaled beak ice conditions, Case 39

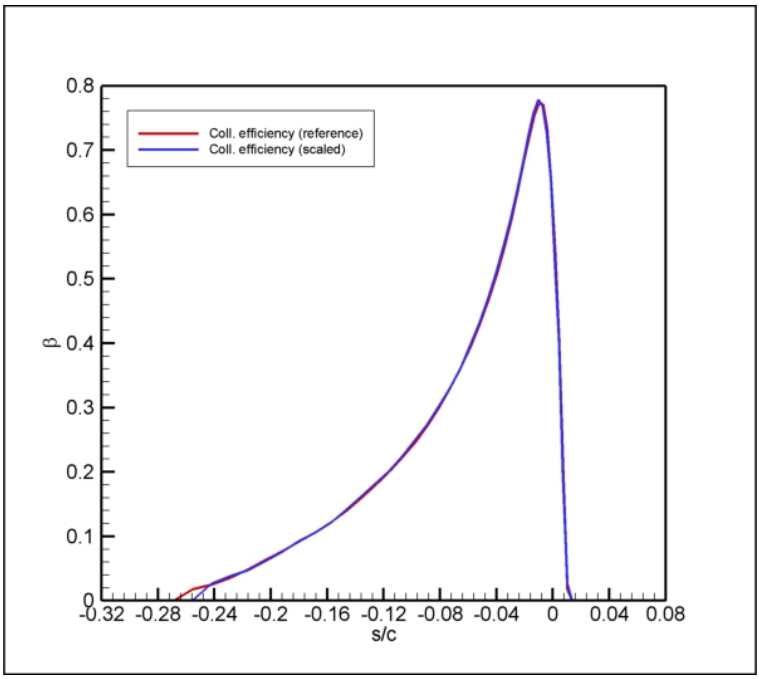

Figure 7: Collection efficiencies for reference and scaled beak ice conditions, Case 39

5 Conclusion

In this study, scaling and icing prediction calculations were applied through a six-parameter Modified Ruff Method similitude and scaling framework. In order to validate the framework, icing cases for rime, glaze and beak ice conditions for a 50% scaled wind-tunnel model were computed. For each case, the parameters K_0, β_0, A_c, ϕ, n_0, and We were matched between the reference and scaled cases. The computational framework was validated by comparing ice shapes and droplet collection efficiency distributions for the reference and scaled conditions.

DOI: 10.13009/EUCASS2025-662

The evaluation of three distinct icing regimes representing rime, glaze, and beak ice conditions demonstrated the reliability and effectiveness of the applied scaling methodology across varying icing regimes. In the case of rime ice, where freezing occurs instantaneously, similitude was primarily governed by droplet trajectory and water catch behavior. Under such less complex conditions, the agreement between model and reference ice shapes was almost exact. For the glaze ice scenario, involving partial freezing and runback effects, achieving similitude required accurate reproduction of energy balance and surface-film dynamics in addition to droplet trajectory and water catch. In the beak ice case, despite the moderately compressible flow conditions (Mach 0.568), panel-method corrections effectively preserved flow-field similitude. The model successfully replicated both the collection efficiency and geometric characteristics of the beak formation, confirming the robustness of the approach even under higher-speed conditions.

The findings of this study confirm that the six-parameter set, complemented by the Weber number, provides a reliable basis for achieving similitude across rime, glaze, and beak icing regimes. The integration of numerical simulations with the Modified Ruff Method algorithm enables effective prediction of scaled icing conditions. Moreover, the results highlight the need for further refinement of the methodology in high-speed, high-temperature scenarios, particularly where compressibility effects and runback water modelling are significant. Overall, the proposed scaling framework offers a validated and practical pathway from computational modeling to experimental verification, ultimately with a potential to support certification of air vehicles or their components subject to in-flight icing conditions. An interesting extension of the methodology would be towards rotating wings, which would require scaling and establishing similitude of the rotational speed. This would enable geometries like propellers and wind turbine blades to be analyzed using the framework developed in the current study.

References

[1] Sibley, E. J. and Smith, R. E., Model Testing in an Icing Wind Tunnel, Lockheed Aircraft Corp., Inc., Report No. LR-10981, 1955.

[2] Dodson, E. D., Scale Model Analogy for Icing Tunnel Testing, Document No. D6-7976, 1962.

[3] Ruff, G.A. 1985 Analysis and Verification of the Icing Scaling Equations, Arnold Engineering Development Center, USAF, AEDC-TR-85-30.

[4] Anderson D.N. 2004 Manual of Scaling Methods, NASA CR-2004-212875.

[5] Jeck, R.K. 2002 Icing Design Envelopes (14 CFR Parts 25 and 29, Appendix C) Converted to a Distance-Based Format, U.S. Department of Transportation, Federal Aviation Administration, Report No: DOT/FAA/AR-00/30.

[6] European Union Aviation Safety Agency 2023 Certification Specifications and Acceptable Means of Compliance for Large Aeroplanes - CS 25, Amendment 27.

[7] Federal Aviation Administration, U.S. Department of Transportation 2023 Airworthiness Standards: Transport Category Airplanes, 14 CFR Part 25, last amended October 2, 2023.

[8] M. G. Potapczuk, Aircraft Icing Research at NASA Glenn Research Center, *Journal of Aerospace Engineering*, vol. 26, no. 2, pp. 260–276, 2013.

[9] Messinger, B.L. 1953 Equilibirum temperature of an unheated icing surface as a function of air speed, *Journal of the Aeronautical Sciences*, Vol. Jan 1953.

[10] M. Tribus, G. B. W. Young, and L. M. K. Boelter, Analysis of heat transfer over a small cylinder in icing conditions on Mount Washington, *Transactions of the American Society of Mechanical Engineers*, vol. 70, no. 8, pp. 971–976, 1948.

[11] Özgen, S. and Canibek, M. 2009 Ice accretion simulation on multi-element airfoils using Extended Messinger Model, *Heat Mass Transfer*, Vol. 45.

[12] Wright, W.B., Gent, R.W. and Guffond, D. 1997 DRA/NASA/ONERA Collaboration on Icing Research, Part II. Prediction of Airfoil Ice Accretion, NASA CR-202349.

[13] Özkanakti, M.H. 2023 Ice accretion simulation and scaling analysis for conceptual design of an icing wind tunnel, Ph. D. dissertation, Middle East Technical University, Dept. Aerospace Eng.

[14] Özgen, S. and Canibek, M. 2012 In-flight icing prediction with high-speed flow effects, *9th International Conference on Heat Transfer, Fluid Mechanics and Thermodynamics, HEFAT 2012*.